

Intelligent Synthesis of Driving Cycle for Advanced Design and Control of Powertrains

Bolin Zhao, Theo Hofman, Chen Lv, *Member, IEEE*, and Maarten Steinbuch, *Senior Member, IEEE*

Abstract— As an important input for the simulation and design process of powertrains, a driving cycle needs to be representative of real-world driving behavior. For the purpose of reducing the time consumption in the simulation, a novel modeling method is required to get a representative short driving cycle from the driving datasets. In this paper, a stochastic model based driving cycle synthesis is introduced. The Markov Chain process is combined with a transition probability extracted from the input driving data to determine the next possible state of the vehicle. Specifically, the velocity and slope are generated simultaneously using a three-dimensional Markov Chain model. After the generation process, the result is validated by selected criteria. Furthermore, this synthesis can generate the driving cycle with the desired length to compress the original driving cycle. The results show that the successful compression of the driving cycle can be tested for the fuel economic in the powertrain simulation. At last, the standard deviation of acceleration is found that has a positive correlation of the compression capability of the driving cycle.

I. INTRODUCTION

The modern vehicle design process is based on modeling and simulations. Driving cycles are the essential input in simulation process used to evaluate fuel consumption standards or other concerns. NEDC, FTP-75, and JN1015 are well-known driving cycles used in such scenarios [1]. As the amount of simulation-based research continues to increase, the current cycles need to be further improved.

In the existing studies, the most commonly used method for driving cycle synthesis is the two-dimensional Markov Chain based on the velocity and acceleration. However, no current research explores the Markov Chain ability to compress driving cycles which benefits for the overall efficient of the simulation. Moreover, owing to the large number of data cluster classes in the current research, it is not feasible to generate the driving cycle online while the vehicle in operation, because transition estimation requires too much time. However, it should be possible to compress logged driving data into a relatively short driving cycle and apply it to predict future driving behavior.

Motivated by the existing research we investigate augmenting the Markov Chain to include slope information in

the synthesized driving cycle. To reduce the simulation time, which is counted in days, with a high combination of the resolution of data, we investigate the possibility of increasing the width of classes. After smoothing is performed during post-processing, the generated cycle is acceptable in terms of the selected criteria. A statistical validation provides overview of the quality of the result. Based on the regression analysis, the relation between the properties of cycle and the compress rate is deduced.

The Outline of this paper is described as follows. In Sections II and III of the paper, it describes the driving cycle synthesis. In Section II, the three-dimensional Markov Chain synthesis is discussed in terms of different numbers of data classes, to indicate the possibility of real-time implementation. Next, in Section III, the influence of the generated cycle time length is considered. Finally, in Section VI, the conclusions on the synthesis and implementations are drawn.

II. DRIVING CYCLE SYNTHESIS

In this section, the synthesis based on the three-dimensional Markov Chain is explained and validated as an efficient method to regenerate the driving cycle. The three-dimensions include velocity, acceleration, and slope. From a statistical point of view, principal component analysis is conducted to ensure that the method is capable of rebuilding the random driving cycle within the selected criteria.

A. Three-dimensional Markov Chain model

Most of the studies do not take slope information into account as described in [2], [3], and [4]. While the regenerative braking is a main benefit and has influence on the performance of the electrified powertrain [1], extracting another two-dimensional Markov Chain for slope is possible. However, the harmony between the generation of the velocity and slope is not reasonable owing to the individual stochastic process. To ensure performance and include the slope information, the widely used Markov Chain model should be extended to a higher dimension. A three-dimension Markov Chain with velocity, acceleration, and slope may solve this problem. The overall structure of the modeling method is reported in Fig. 1. It consists of three parts: 1) Extract the transition matrix T and transition probability matrix F from the database; 2) Generate the new sample from transition matrix T ; 3) Smoothing the result for mean tractive force. After these above steps, the time-domain driving cycle is transformed into a time-invariant statistical model.

B. Validation of the Methodology

To validate the method can generate a candidate cycle with the same quality as the original one, the following statistical criteria are used: stand deviation of the velocity, average velocity, maximal velocity, standard deviation of the

* This research was partially supported by the Young Elite Scientific Sponsorship Programme of China Association for Science and Technology (CAST), Project No. 2017QNRC001.

Bolin Zhao is with Ricardo Limited Company, Shanghai, China (e-mail: bolin.zhao@ricardo.com).

Theo Hofman and Maarten Steinbuch are with the Department of Mechanical Engineering, Eindhoven University of Technology, Eindhoven, The Netherlands (e-mail: t.hofman@tue.nl, m.steinbuch@tue.nl).

Chen Lv is with the School of Mechanical and Aerospace Engineering and the School of Electrical and Electronic Engineering, Nanyang Technological University, Singapore (e-mail: henrylvchen@gmail.com).

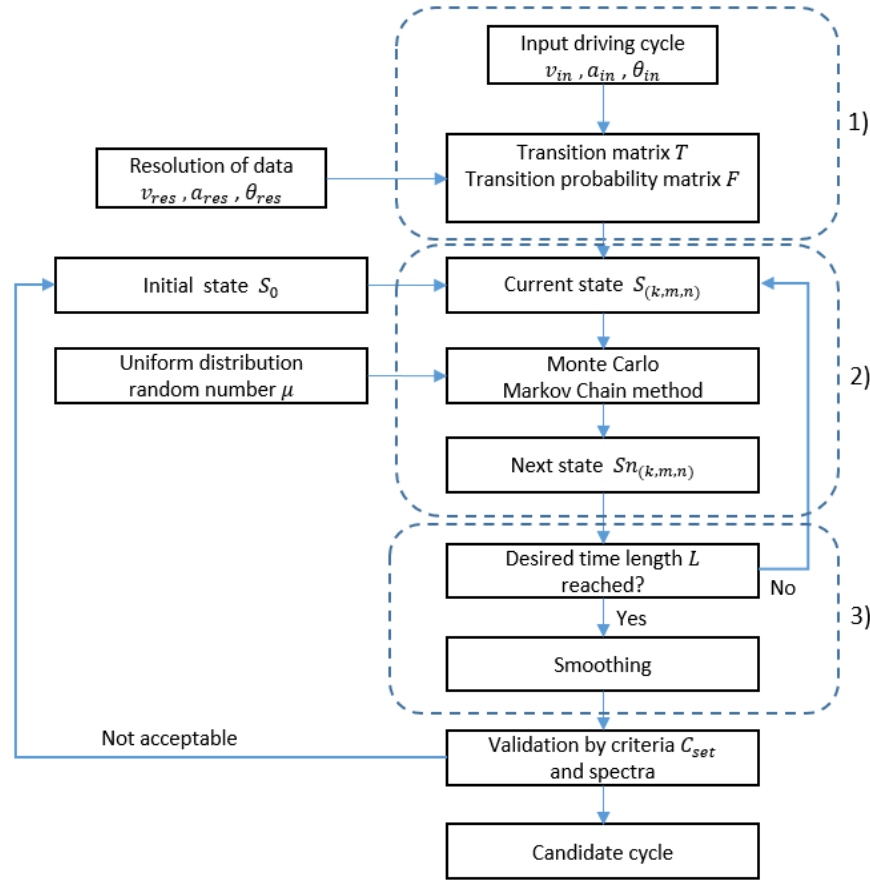


Figure 1. Overall structure of the Markov Chain method.

acceleration, maximal acceleration, and minimal acceleration. These criteria are listed in Table I. The criteria set is defined as Eq. (2). Kinds of possible criteria are discussed in [5], [6] and [7].

TABLE I. SELECTED CRITERIA FOR THE GENERATED CYCLE

Symbol	Meaning	Unit
V_{std}	Standard deviation of velocity	m/s
V_{max}	maximal velocity	m/s
V_{avg}	average velocity	m/s
A_{std}	standard deviation of acceleration	m/s^2
A_{max}	maximal acceleration	m/s^2
A_{min}	minimal acceleration	m/s^2
θ_{std}	standard deviation of slope	deg
θ_{max}	maximal slope	deg
θ_{min}	minimal slope	deg

The standard deviation is defined as Eq. (1). The mean value of the variable is \bar{X} . The total sample number of the variable is N .

$$X_{std} = \sqrt{\frac{1}{N} \sum_{i=1}^N (X_i - \bar{X})^2} \quad (1)$$

$$C_{set} = [V_{std}; V_{max}; V_{avg}; A_{std}; A_{max}; \theta_{std}; \theta_{max}; \theta_{avg}] \quad (2)$$

Moreover, an acceptable candidate cycle should be easily reached for this synthesis. The 1000 random generations are extracted from the synthesis and the overall statistical performance is reported. The criteria of the input cycle are denoted by C_{in} . For each random generation, the criteria in C_{gen} is calculated and normalized using the target value C_{in} . The normalized difference between the criteria and the original cycle is C_{rel} .

$$C_{rel} = \frac{|C_{gen} - C_{in}|}{C_{in}} \cdot 100\% \quad (3)$$

The principal components analysis analyzes the contributing effect of the individual criteria in the criteria set. The principal components analysis shows that the first three principle components contribute more than 95% of the variance. This indicates that the first three principle components are the most important variables, and that they can reflect the difference between generations effectively. Furthermore, the transfer principle components still stand for the normalized difference value. Then, a K-means cluster method [8] divides the three principle components into three classes, as shown in Fig. 2. The centroids of the cluster 1, 2,

and 3 are (-8.16%, -13.70%, 7.50%), (-46.44%, -15.97%, -3.05%), and (35.40%, -16.77%, -3.31%), respectively.

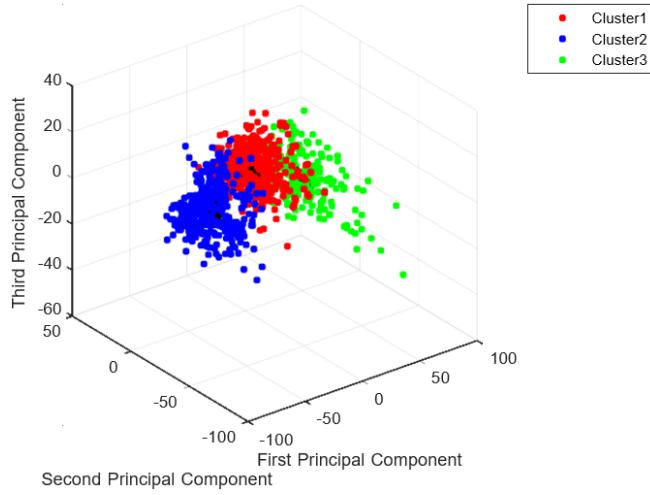


Figure 2. Three clusters for 1000 generations after principle components analysis.

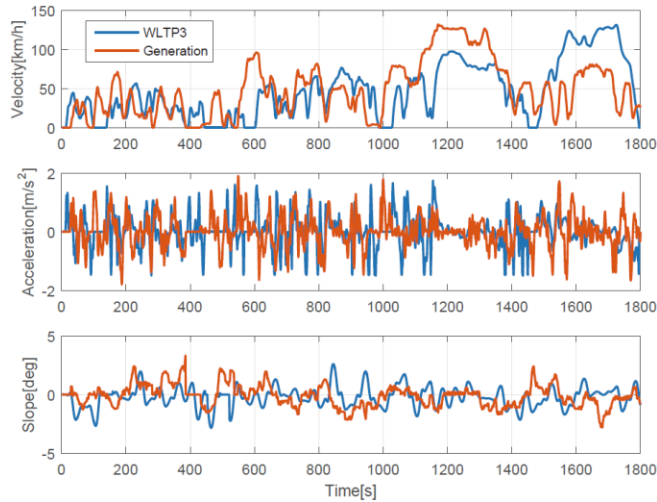


Figure 3. An acceptable candidate cycle generated by the de-signed method.

The first centroid is closest to the original point which means the cycles in this cluster differ the least from the original cycle. The figure shows that the red points gather around the original point. Furthermore, the counts in each cluster are 436, 198 and 196. This indicates that the three-dimensional Markov Chain method can reliably generate a candidate cycle with similar properties within a 15% difference. The overall condition of the acceptable result is defined as Eq. (4).

$$C_{rel} \leq 15\% \quad (4)$$

An example of an acceptable generation, which was obtained from cluster 1, is presented in Fig. 3. The difference in the statistical results are listed in Table II. If the low-frequency range (< 0.1 Hz) is attributed to traffic conditions [9], the performance is almost the same. In the higher frequencies, the difference is significant owing to the smoothing process, which constrains the high-frequency fluctuation of the velocity.

TABLE II. DIFFERENCES IN CRITERIA FROM A CANDIDATE CYCLE

Criteria	Deviation Values from the Input Cycle (%)
Mean Velocity	3.37
Standard deviation velocity	2.14
Maximal Velocity	1.52
Maximal Slope	-11.98
Minimal Slope	0.11
Standard deviation Acceleration	8.32
Minimal Acceleration	16.19

III. DRIVING CYCLE COMPRESSION

Driving cycle compression is of great importance for the development of industrial mechatronic systems and ground vehicle. The typical short-term driving cycle are widely used in the design and validation process as shown in [10], [11] and [12]. In this section, the time length of the generated cycle will be controlled to explore the possibility of generating a shorter cycle.

A. Generation for compressed time lengths

The degrees of freedom of the Markov Chain process in this study depend on the generated cycle time length L and the combined resolutions a_{res} , v_{res} , and θ_{res} . From the discussion in the previous section, a combined resolution configuration is given as 2.22 m/s, 0.2 m/s² and 0.5° . The generating cycle length L is defined by the user. The longer the length is, the more time it will take in the generating and simulation process. To explore the influence of the time length during the generation, 11 lengths are chosen in this study as Eq. (5).

$$L = \{180, 360, 540, 720, 900, 1080, \dots, 1260, 1440, 1620, 1800, 2700\} \quad (5)$$

The desired time length of the cycle is the minimum time length needed to successfully retain the properties of the original driving cycle. For each time length, 200 times generations are made to found out the statistical properties.

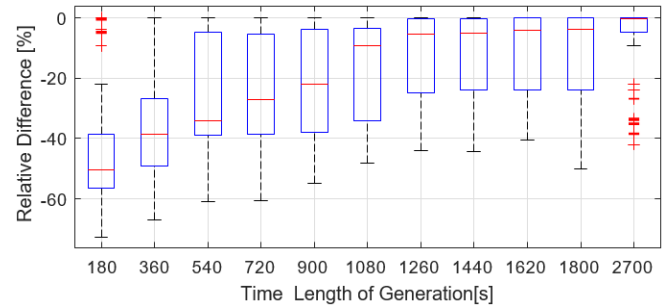


Figure 4. Relative differences in standard deviation of the velocities for various generating lengths.

Fig. 4 provides a brief view of the influence of generating length on velocity. The original time length of the data is 1800 s. The first observation is that the difference in the standard deviation of the velocity decreases with increases in

generating length. A generated length that is no less than 50% of the original length can reliably generate a new cycle with the same standard deviation of velocity. The results of the 1.5 times the original length are good evidence. The median is close to 0 which means the most frequent results exhibit the same performance as the original result. The second observation is that the values of most of the results with different time lengths are lower than the desired value, especially for the short period generations. The ranges of the differences for each length are approximately 30%.

Three typical results from generations of 900 s, 1440 s, and 1800 s are presented in Fig. 5. For generations with time lengths of less than 900 s, the maximum velocity is likely less than 100 km/h. This phenomenon is due to a transition started from the idle state. With a fixed sample time and resolution, it is relatively important that the top speed will be reached in the minimum time. The longer the generation time, the higher the probability that the top speed will be reached. From this point of view, taking all the differences into account, the maximum acceptable compression ratio for the WLTP3 cycle is 50% to ensure a fast generation.

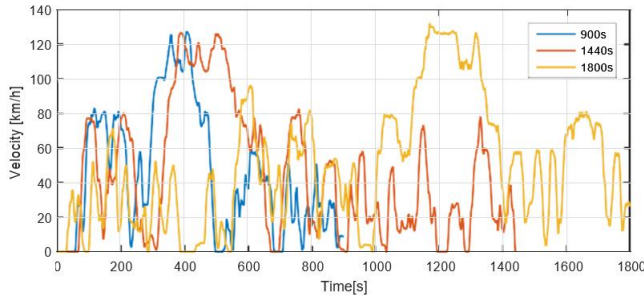


Figure 5. Three typical generations with different lengths.

To implement the Markov Chain driving cycle synthesis into the design process of hybrid electric vehicle (HEV), a parallel hybrid vehicle model equipped with the equivalent consumption minimization strategy (ECMS) [13] is introduced.

B. Effect of driving cycle compression on powertrains

Driving cycle is of great importance for vehicle and powertrain design, control and optimization [14-19]. In this section, a method to transfer long-term driving data into a short-term driving cycle using designed synthesis will be discussed.

Different types of combination tests have been conducted using a variety of models. First of all, three HEV models as shown in Table III in the WLTP3 driving cycle are determined to establish fundamental values for research. The equivalence factor of each combination is retuned to maintain the terminal state of charge at 69.95% to 70.05%. From Table IV, the hybrid powertrain is proved to reduce the fuel consumption.

To investigate the performance of the cycle generation tool described in the previous section, the powertrains are also tested using the compressed driving cycles.

If differences in the criteria of the compressed cycle and original cycle are not larger than 15%, the generation is acceptable. In the 2000 generations for various time lengths, only some of them are accepted; an example is shown in Fig.

6. Then, the conventional vehicles and hybrid vehicles are tested using the acceptable result, in order to determine the fuel consumption. The results are reported in Fig. 7. The dashed lines in the figures show the upper and lower boundaries representing a 10% difference from values listed in Table IV. The compressed ratio α in this case is based on Eq. (6). The time length of the generation is L_{gen} , and L_{wlp3} is the time length of the WLTP3 cycle.

TABLE III. DIFFERENCES IN CRITERIA FROM A CANDIDATE CYCLE

Hybrid Vehicle	Lux Sedan	SUV	Sedan
Internal Combustion Engine Maximal Power (kW)	130	155	95
Engine Maximal Torque (Nm)	183	220	150
Electric Motor (kW)	35	35	35
Maximal Torque (Nm)	130	130	130
Battery (Ah)	6	6	3
Total Mass (kg)	1590	1978	1355
Road Resistance [-]	0.013	0.015	0.012
Drag Coefficient [-]	0.32	0.35	0.32
Drag Area (m ²)	2.2	2.5	2.0
Radius of Tire (m)	0.3	0.3	0.3

TABLE IV. FUEL CONSUMPTION IN WLTP3

Model	WLTP3 (L/100km)
Sedan	7.75
Hybrid Sedan	3.11
Equivalence Factor β	2.66
Lux Sedan	10.43
Hybrid Lux Sedan	4.03
Equivalence Factor β	3.34
SUV	14.94
Hybrid SUV	6.07
Equivalence Factor β	4.50

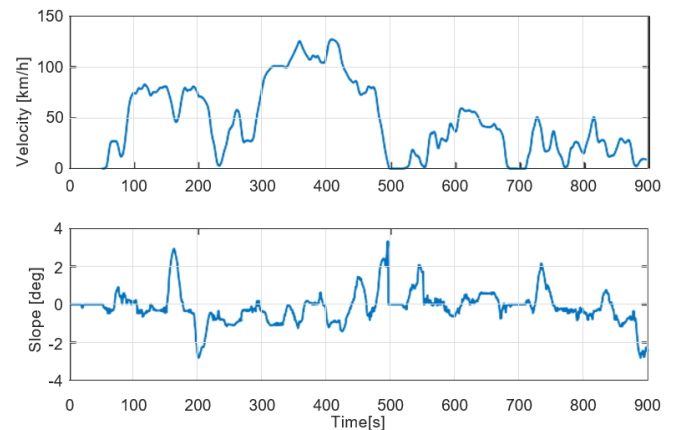


Figure 6. A successful compressed cycle with 50% time length.

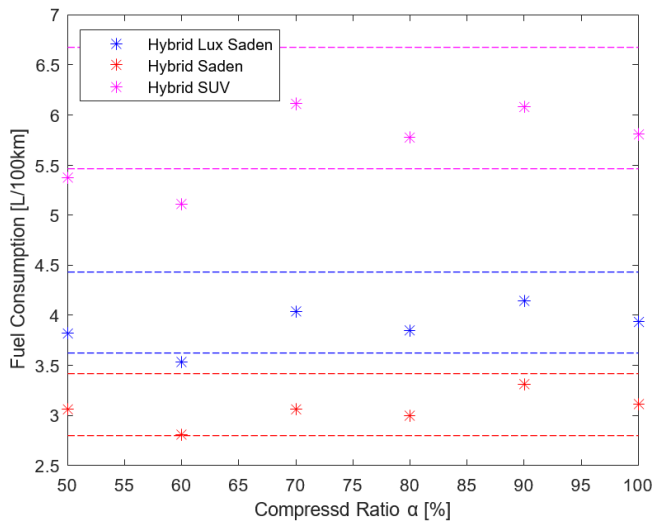


Figure 7. Fuel consumption in compressed driving cycles for different types of hybrid vehicles (dashed line represent 10% upper and lower boundaries).

$$L_{gen} = \alpha \cdot L_{wlp3} \quad (6)$$

$$\alpha \in (0, 100\%]$$

From the figures, it is clear that most of the results are located in the 10% boundaries. Furthermore, the higher the compression rate, the more difficult it is to produce an accept-able result for the criteria.

C. Minimum acceptable compression rates for different drive cycles

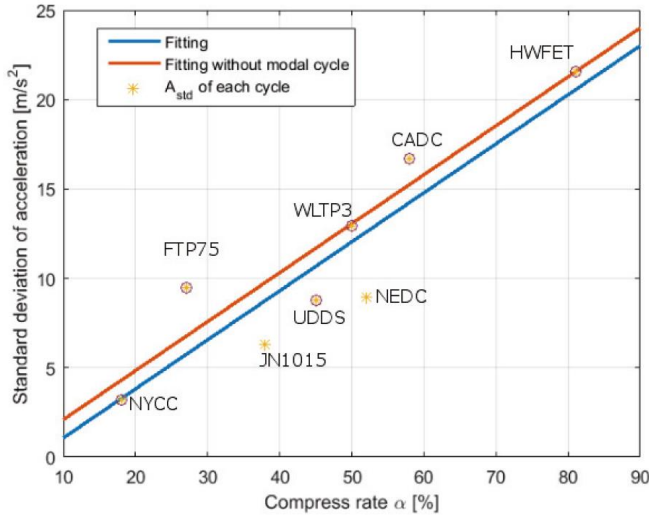


Figure 8. Regression analysis for the standard deviation of the acceleration.

To find out which property of the input cycle affects the compression ability, eight standard driving cycles are compressed by the synthesis. Two of them are modal driving cycle (NEDC and JN1015), the else are transient (WLTP3, FTP75, NYCC, UDDS, US06, CADC, and HWFET). The regression analysis for the selected criteria shows that only the standard deviation of acceleration of the original cycles has a strong linear relation ($R^2=0.8152$). And if only the transition cycles are taken into account, the quality of fitting will be improved ($R^2=0.9075$). The relation between the standard

deviation of acceleration and compress rate is shown in Fig. 8. It can be seen that the higher standard deviation of acceleration the cycles, the more difficult the compression will be conducted.

The above results show that under the defined configuration, the compressed rate can be 50% at most. The influence of compression becomes more significant as the size of the engine increases. However, increasing either the size of the database or the combined resolution of velocity, acceleration and slope may lead to better performance for the compressed cycle.

IV. CONCLUSION

In this paper, we introduce a three-dimensional Markov Chain method that obtains the stochastic model from the existing driving cycle. The model effectively works with the Monte Carlo method to generate a new driving cycle and of the same length while retaining similar properties. It is also possible to accurately and efficiently compress the WLTP3 cycle down to 50% of its original length. The acceptable compress rate is varied by the original length and the complexity of the original cycle. Meanwhile, it is possible to design a conventional powertrain based on the compressed cycle, but for hybrid powertrains, especially heavy-duty ones, a compressed cycle with a compression rate less than 70% is not reliable with the current configuration. The maximum compress rate of a given cycle is based on the standard deviation of the acceleration. It indicates that the relatively smoothing driving cycle has more potential to be compressed.

ACKNOWLEDGMENT

This work was partially supported by the Young Elite Scientific Sponsorship Programme of China Association for Science and Technology (CAST), Project No. 2017QNRC001.

REFERENCES

- [1] C. Lv, J. Zhang, Y. Li, and Y. Yuan, "Mechanism analysis and evaluation methodology of regenerative braking contribution to energy efficiency improvement of electrified vehicles," *Energy Conversion and Management*, vol. 92, no. 469-482, 2015..
- [2] T.-K. Lee, B. Adornato, and Z. S. Filipi, "Synthesis of real-world driving cycles and their use for estimating PHEV energy consumption and charging opportunities: Case study for midwest/U.S." *IEEE Transaction on Vehicular Technology*, vol. 60, 2011.
- [3] S. Shi, S. Wei, H. Kui, L. Liu, C. Huang, and M. Liu, "Improvements of the design method of transient driving cycle for passenger car," in 2009 IEEE Vehicle Power and Propulsion Conference, 2009.
- [4] Q. Gong, S. Midlam-Mohler, V. Marano, and G. Rizzoni, "An iterative markov chain approach for generating vehicle driving cycles," *SAE International Journal of Engines*, 2011.
- [5] P. Nyberg, E. Frisk, and L. Nielsen, "Generation of equivalent driving cycles using markov chains and mean tractive force components," 19th IFAC World Congress, 2014.
- [6] T.-K. Lee and Z. S. Filipi, "Synthesis of real-world driving cycles using stochastic process and statistical methodology," *International journal of vehicle design*, vol. 57, no. 1, pp. 17-36, 2011.
- [7] W. Hung, H. Tong, C. Lee, K. Ha, and L. Pao, "Development of a practical driving cycle construction methodology: A case study in hong kong" *Transportation Research Part D: Transport and Environment*, vol. 12, no. 2, pp. 115-128, 2007.

- [8] A. Fotouhi and M. Montazeri-Gh, "Tehran driving cycle development using the k-means clustering method," *Scientia Iranica*, vol. 20, no. 2, pp. 286–293, 2013.
- [9] Z. Liu, A. Ivanco, and Z. S. Filipi, "Impacts of real-world driving and driver aggressiveness on fuel consumption of 48v mild hybrid vehicle," *SAE International Journal of Alternative Powertrains*, vol. 5, no. 2016-01-1166, 2016.
- [10] C. Lv, Y. Liu, and et al, "Simultaneous observation of hybrid states for cyber-physical system: a case study of electric vehicle powertrain," *IEEE Transactions on Cybernetics*, 2017, in press.
- [11] C. Lv, H. Wang, and D. Cao, "High-precision hydraulic pressure control based on linear pressure-drop modulation in valve critical equilibrium state," *IEEE Transactions on Industrial Electronics*, 2017, in press.
- [12] C. Lv, J. Zhang, Y. Li, and Y. Yuan, "Novel control algorithm of braking energy regeneration system for an electric vehicle during safety-critical driving maneuvers," *Energy Conversion and Management*, vol. 106, no. 520-529, 2015..
- [13] G. Paganelli, S. Delprat, T.-M. Guerra, J. Rimaux, and J.-J. Santin, "Equivalent consumption minimization strategy for parallel hybrid powertrains," in *Vehicular Technology Conference, 2002. VTC Spring 2002. IEEE 55th*, vol. 4. IEEE, 2002, pp. 2076–2081.
- [14] C. Lv, D. Cao, Y. Zhao, D. J. Auger, et al., "Analysis of autopilot disengagements occurring during autonomous vehicle testing," *IEEE/CAA Journal of Automatica Sinica*, vol. 5, pp. 58-68, 2018.
- [15] C. Lv, Y. Xing, J. Zhang, X. Na, Y. Li, T. Liu, et al., "Levenberg-Marquardt Backpropagation Training of Multilayer Neural Networks for State Estimation of A Safety Critical Cyber-Physical System," *IEEE Transactions on Industrial Informatics*, 2017
- [16] J. Zhang, C. Lv, et al. "Cooperative control of regenerative braking and hydraulic braking of an electrified passenger car." *Proceedings of the Institution of Mechanical Engineers, Part D: Journal of Automobile Engineering* 226, no. 10 (2012): 1289-1302.
- [17] C. Lv, H. Wang, D. Cao, Y. Zhao, D. J. Auger, M. Sullman, et al., "Characterization of Driver Neuromuscular Dynamics for Human-Automation Collaboration Design of Automated Vehicles," *IEEE/ASME Transactions on Mechatronics*, 2018, in press.
- [18] C. Lv, Y. Xing, C. Lu, Y. Liu, H. Guo, H. Gao, et al., "Hybrid-Learning-Based Classification and Quantitative Inference of Driver Braking Intensity of an Electrified Vehicle," *IEEE Transactions on Vehicular Technology*, 2018, in press.
- [19] Zhao, B., Lv, C., Hofman, T., Steinbuch, M. et al., "Design Optimization of the Transmission System for Electric Vehicles Considering the Dynamic Efficiency of the Regenerative Brake," *SAE Technical Paper 2018-01-0819*, 2018.